bonds between molecules. More important, the two different chemical shifts of the sp^3 carbons directly confirm the results of our structural refinement—that is, the symmetry inequivalence of the two carbon atoms bridging neighboring molecules in the polymeric chains. Deconvolution of the spectrum in the sp^2 region between 130 and 160 ppm with Lorentzians reveals seven peaks, as compared to five peaks for the monomeric species, and is a further manifestation for cage deformation upon polymerization.

Although the C_{70} polymer crystal is stable at ambient conditions, it reverts to the monomeric state upon heating at ambient pressure, much like C_{60} polymers. Our dilatometric experiments on the single-crystal sample of the C_{70} polymer (*31*) indicate the onset of depolymerization as an abrupt increase of sample dimensions starting at about 450 K. Upon completion of this process, the orientational order-disorder transitions characteristic of molecular dynamics in the monomeric C_{70} are restored and the Raman spectrum of the material is identical to that of pristine C_{70} (Fig. 1A).

Our results demonstrate how nature solves the seeming problem of incompatible molecular (fivefold) and crystal (sixfold) symmetries of C_{70} by forming zigzag polymer chains. The topochemical polymerization is governed by the packing of molecules in C_{70} crystal and indicates that the system topology must play a key role in the polymerization of higher fullerenes and formation of 3D networks of cross-linked fullerene cages.

References and Notes

1. V. D. Blank *et al.*, *Phys. Lett. A* **205**, 208 (1995).
2. L. Marques *et al.*, *Science* **283**, 1720 (1999).
3. S. Okada, S. Saito, A. Oshiyama, *Phys. Rev. Lett.* **83**, 1986 (1999).
4. V. D. Blank *et al.*, *Phys. Lett. A* **248**, 415 (1998).
5. A. M. Rao *et al.*, *Science* **259**, 955 (1993).
6. Y. Iwasa *et al.*, *Science* **264**, 1570 (1994).
7. M. Nunez-Regueiro, L. Marques, J.-L. Hodeau, O. Bethoux, M. Perroux, *Phys. Rev. Lett.* **74**, 278 (1995).
8. B. Sundqvist, *Adv. Phys.* **48**, 1 (1999).
9. R. Moret, P. Launois, P.-A. Persson, B. Sundqvist, *Europhys. Lett.* **40**, 55 (1997).
10. G.-W. Wang, K. Komatsu, Y. Murata, M. Shiro, *Nature* **387**, 583 (1997).
11. R. Moret, P. Launois, T. Wågberg, B. Sundqvist, *Eur. Phys. J. B* **15**, 253 (2000).
12. N. Chandrabhas *et al.*, *Phys. Rev. Lett.* **73**, 3411 (1994).
13. A. M. Rao *et al.*, *Chem. Phys. Lett.* **224**, 106 (1994).
14. C. S. Sundar *et al.*, *Phys. Rev. B* **53**, 8180 (1996).
15. Y. Iwasa *et al.*, *Appl. Phys. A* **64**, 251 (1997).
16. M. Premila *et al.*, *Solid State Commun.* **104**, 237 (1997).
17. S. Lebedkin, W. E. Hull, A. Soldatov, B. Renker, M. M. Kappes, *J. Phys. Chem. B* **104**, 4101 (2000).
18. J. Baker, P. W. Fowler, P. Lazzeretti, M. Malagoli, R. Zanasi, *Chem. Phys. Lett.* **184**, 182 (1991).
19. G. B. M. Vaughan *et al.*, *Chem. Phys.* **178**, 599 (1993).
20. M. A. Verheijen *et al.*, *Chem. Phys.* **166**, 287 (1992).
21. S. van Smaalen *et al.*, *Chem. Phys. Lett.* **223**, 323 (1994).
22. A. V. Dzyabchenko, V. Agafonov, V. A. Davydov, *J. Phys. Chem. A* **103**, 2812 (1999).
23. M. Haluska *et al.*, *Appl. Phys. A* **56**, 161 (1993).
24. P. A. Persson *et al.*, *Chem. Phys. Lett.* **258**, 540 (1996).
25. L. Speck et al., *Program System PLATON* (Bijvoet Center for Biomolecular Research, University of Utrecht, Utrecht, Netherlands, 1999).
26. For supplementary data on parameter values, atomic coordinates, bond lengths, with further details of the refinement and modeling of polymeric and dimeric structures of C_{70}, see *Science* Online (www.sciencemag.org/cgi/content/full/293/5530/680/DC1).
27. A. Soldatov, B. Sundqvist, *J. Phys. Chem. Solids* **57**, 1371 (1996).
28. M. J. Frisch *et al.*, Gaussion 98W (Gaussian Inc., Pittsburgh, PA, 1998).
29. The FTIR spectrum of the powder material is similar to that of the single-crystal C_{70} polymer and indicates the fraction of C_{70} dimers less than 15%. The number of stacking faults in the powder is substantially larger than in the single crystal, which results in shorter polymeric chains. Nonetheless, this should not influence the characteristic features of the NMR spectrum of the polymer.
30. C. Goze *et al.*, *Phys. Rev. B* **54**, R3676 (1996).
31. A. Soldatov, P. Nagel, C. Meingast, unpublished data.

32. We thank S. Balibar, A. Bezryadin, E. Campbell, J. Fischer, Y. Iwasa, I. Silvera, and H. Suga for critical reading of the manuscript and valuable comments. A.S. gratefully acknowledges the Department of Physics, Umeå University, for support and for providing the experimental facilities for high-pressure synthesis. Further support is acknowledge from the Russian Foundation for Basic Research (A.D.) and by European Community project ERBFMRXCT970155 and Fonds zur Förderong de Wisenschaftlichen Forschung in Austria project P11943 (H.K.).

9 April 2001; accepted 15 June 2001

Calibration of the Lutetium-Hafnium Clock

Erik Scherer,* Carsten Münker, Klaus Mezger

Well-defined constants of radioactive decay are the cornerstone of geochronology and the use of radiogenic isotopes to constrain the time scales and mechanisms of planetary differentiation. Four new determinations of the lutetium-176 decay constant (λ^{176}Lu) made by calibration against the uranium-lead decay schemes yield a mean value of $1.865 \pm 0.015 \times 10^{-11}$ year^{-1}, in agreement with the two most recent decay-counting experiments. Lutetium-hafnium ages that are based on the previously used λ^{176}Lu of 1.93×10^{-11} to 1.94×10^{-11} year^{-1} are thus ~4% too young, and the initial hafnium isotope compositions of some of Earth's oldest minerals and rocks become less radiogenic relative to bulk undifferentiated Earth when calculated using the new decay constant. The existence of strongly unradiogenic hafnium in Early Archean and Hadean zircons implies that enriched crustal reservoirs existed on Earth by 4.3 billion years ago and persisted for 200 million years or more. Hence, current models of early terrestrial differentiation need revision.

Estimates of the timing of dynamic processes in Earth and other planets are almost entirely based on radioactive decay systems that have half-lives between 10^5 and 10^{12} years. The Lu-Hf system, with a half-life of ~37 billion years, is both a versatile geochronometer and a powerful tool for studying the processes that control crust-mantle evolution. However, knowledge of the exact value of the decay constant for the β^--decay of ^{176}Lu to ^{176}Hf is vital to the correct interpretation of Lu-Hf data. The precision and accuracy of both Lu-Hf ages and initial Hf isotope compositions [$\varepsilon_{\mathrm{Hf}}(t)$, (*1*)] depend directly on λ^{176}Lu. The first widely used Lu decay constant, $1.94 \pm 0.07 \times 10^{-11}$ year^{-1}, was derived from the slope of a Lu-Hf isochron for eucrite meteorites of known age (*2*, *3*). This value, based on age comparison, was used until 1997, when a more precise value [$1.93 \pm 0.03 \times 10^{-11}$ year^{-1}, (*4*)] obtained by decay counting was adopted (*5*). However, all other decay-counting experiments made since 1980 (*6*–*10*) yield lower values. The recommended (*10*) mean of recent decay-counting results, $1.86 \pm 0.01 \times 10^{-11}$ year^{-1} (*7, 9, 10*), is ~4% lower than both of the aforementioned decay constants. The accurate application of Lu-Hf systematics requires the reconciliation of decay constants determined from both decay-counting and age-comparison experiments.

Agreement between the two most recent decay-counting results (*9, 10*) is due to the elimination of several experimental difficulties related to (i) optimizing detector geometry and calibration, (ii) knowing the exact amount of ^{176}Lu in the sample, and (iii) correcting for the effects of gamma-ray attenuation, true-coincidence summing, and internal conversion (*10*). Age-comparison studies of minerals and rocks (*2, 3, 11*), in which λ^{176}Lu is calibrated against the relatively well-constrained U decay constants, have been limited by difficulties with measuring Hf isotope compositions and Lu concentrations by thermal ionization mass spectrometry (TIMS). Here, we measured Lu and Hf isotope ratios using multiple-collector inductively coupled plasma mass spectrometry

---

Institut für Mineralogie, Universität Münster, Corrensstrasse 24, 48149 Münster, Germany.

*To whom correspondence should be addressed. E-mail: escherer@nwz.uni-muenster.de

(MC-ICP-MS). This method allows high-precision analyses of small samples (as low as 5 ng of Hf) that were not possible in previous TIMS-based age-comparison studies.

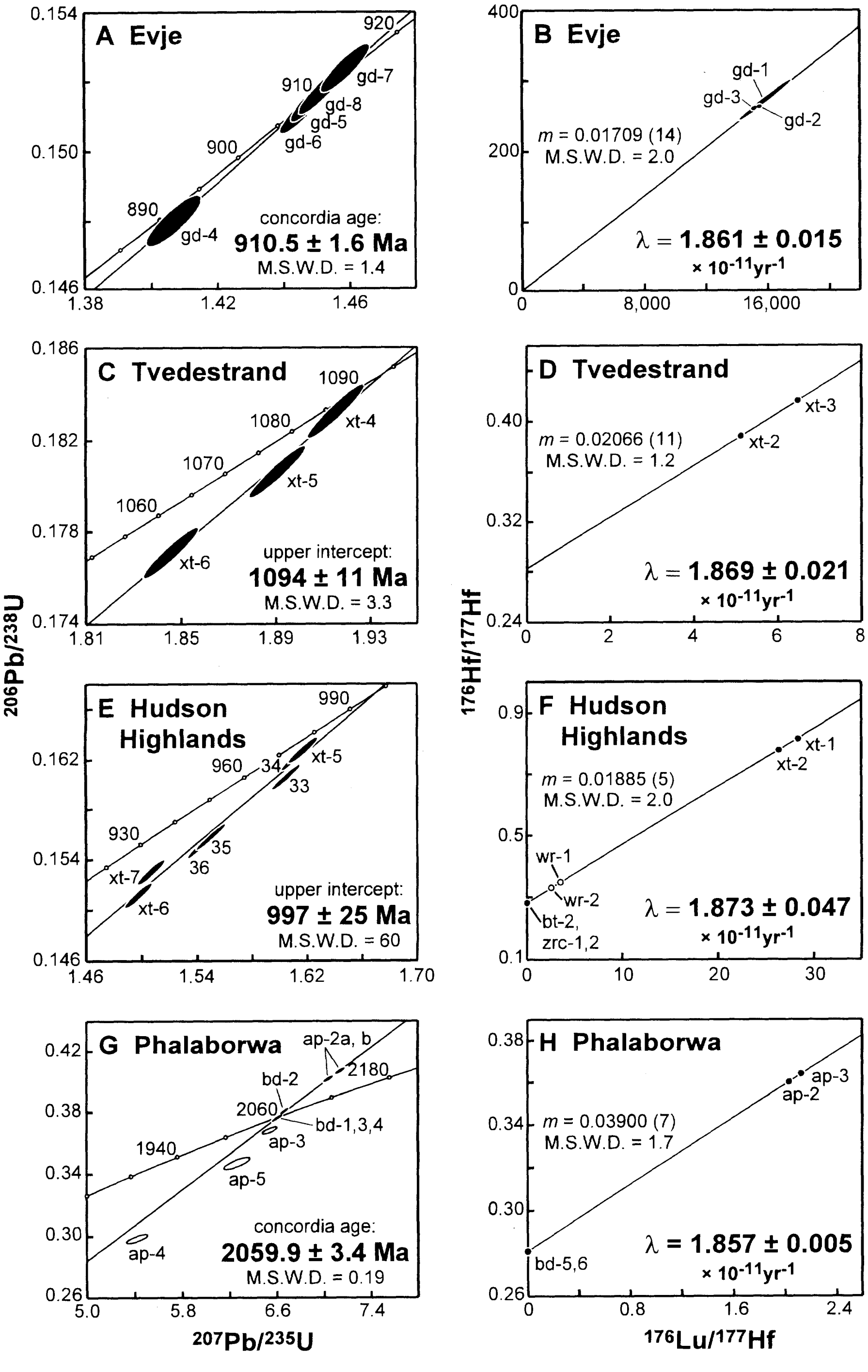

Fig. 1. U-Pb concordia and Lu-Hf isochron diagrams (**A** through **H**). gd, gadolinite; xt, xenotime; ap, apatite; bd, baddeleyite. Open symbols are excluded from the regressions. U-Pb data are available online (*47*). Uranium decay constants: $\lambda^{238}U = 1.55125 \pm 0.00166 \times 10^{-10}$ year^{-1}, $\lambda^{235}U = 9.8485 \pm 0.0134 \times 10^{-10}$ year^{-1} [(*48*); 95% confidence level]. All regressions are model 1 fits (i.e., points weighted according to the inverse square of their errors) except for the Hudson Highlands U-Pb, which is a model 2 fit (i.e., points weighted equally). MSWD statistics of concordia ages (*49*) are for combined equivalence and concordance. Lu-Hf errors are smaller than the symbols, except for Evje where depicted by error ellipses. $\lambda^{176}Lu = \ln(m + 1)/t$, where m is the slope of the Lu-Hf isochron and t is the U-Pb age of the sample in years. Uncertainties on $\lambda^{176}Lu$ values are derived from the 2 SD uncertainties in t and m using $\sigma_\lambda = [\sigma_m^2(\partial\lambda/\partial m)^2 + \sigma_t^2(\partial\lambda/\partial t)^2]^{0.5}$.

Geologic samples for λ^{176}Lu calibration by age comparison were selected according to the following criteria: (i) They must contain minerals highly enriched in the parent elements for both Lu-Hf and U-Pb dating methods. (ii) They must have cooled rapidly, so that the potential effects of differing closure temperatures (T_C) between the Lu-Hf and U-Pb systems or among different minerals are minimized. (iii) The samples should have remained closed systems with respect to Lu-Hf and U-Pb systems since formation. We note, however, that the last criterion does not necessarily have to be met in the strict sense for the U-Pb system. Lead loss or changes in U content, provided they are recent, will not affect ^{207}Pb/^{206}Pb ages. Single, ancient Pb-loss events will produce a discordia whose upper intercept indicates the time of crystallization.

We analyzed a ~100-cm^3 gadolinite crystal from a pegmatite at Evje, Norway, a ~1-cm^3 xenotime crystal from a pegmatite at Tvedestrand, Norway, xenotime from a monazite-xenotime gneiss in the Hudson Highlands, New York, USA, and apatite and baddeleyite from a coarsely crystalline carbonatite from the Phalaborwa intrusion, South Africa (*12*). The Hudson Highlands gneiss probably formed by short-lived metasomatic processes (*13*), and the other minerals come from rapidly cooled intrusions. Though minerals from all four localities were previously dated by the U-Pb system, additional U-Pb TIMS analyses were made to verify the ages of the samples used in the present study. All U-Pb ages and errors that were used to calculate λ^{176}Lu values contain the propagated uncertainties of the U decay constants (*14*).

Five fragments of the Evje gadolinite crystal (EVJ) define a U-Pb upper intercept age of 909 ± 14 million years (Ma), and a cluster of four concordant analyses (gd-5, gd-6, gd-7, and gd-8) gives a concordia age of 910.5 ± 1.6 Ma (Fig. 1A). These ages agree with the 901 ± 20 Ma ^{207}Pb/^{206}Pb age for another gadolinite from the Evje-Iveland area (*11*). Three fragments of the EVJ gadolinite have the most radiogenic Hf yet measured in a natural sample (^{176}Hf/^{177}Hf = 260 to 272, Table 1 and Fig. 1B); 99.9% of the ^{176}Hf was produced by ^{176}Lu decay in the gadolinite crystal. The slope of the Lu-Hf isochron is thus insensitive to the assumed initial ^{176}Hf/^{177}Hf [i.e., that of depleted mantle at 910 Ma, ±20 ε-units (*15*)] that is used as a fourth point in the regression. Although the errors on ^{176}Lu/^{177}Hf and ^{176}Hf/^{177}Hf for the gadolinites are larger than those normally achieved for less radiogenic minerals (*16*), these errors are correlated and therefore the slope of the Lu-Hf isochron is relatively well constrained (±0.8%).

The Tvedestrand xenotime (TVS) comes from a pegmatite that intruded into a regionally cooling terrane (the Bamble sector of southern Norway) whose temperature at the time of intrusion is constrained by hornblende ^{40}Ar/^{39}Ar ages [(*17*) and references therein] to be ≤600°C. The T_C for U-Pb in xenotime is similar to that of monazite [(*13, 18*); i.e., ~725°C (*19*)] or higher [≥800°C (*20*)], and thus the

U-Pb age for sample TVS is taken to be the crystallization age. Three xenotime fragments define a U-Pb chord that has an upper intercept at 1094 ± 11 Ma (Fig. 1C). The minor apparent Pb loss in these fragments was assumed to have occurred during heating associated with magmatism in the Permian Oslo Rift; allanite and zircon from the Bamble sector exhibit similar Permian Pb-loss patterns (*17, 21*). The lower intercept was therefore anchored at 280 ± 50 Ma. Removing this constraint results in an identical xenotime age of 1094 +76/−17 Ma. Though less radiogenic than the EVJ gadolinite, two TVS xenotime fragments have sufficiently elevated $^{176}\text{Lu}/^{177}\text{Hf}$ and $^{176}\text{Hf}/^{177}\text{Hf}$ ratios, and they lie on an isochron that uses a range of possible initial $^{176}\text{Hf}/^{177}\text{Hf}$ ratios [i.e., depleted mantle at 1094 Ma, ±20 ε-units (*15*)] as a third point (Fig. 1D).

Three U-Pb analyses of single xenotime grains from the Hudson Highlands gneiss (RS-1) are plotted in Fig. 1E together with previously published (*13*) xenotime analyses from the same outcrop. Aleinikoff and Grauch (*13*) excluded one of four analyses from their discordia regression and report a xenotime age of 986.5 ± 1.5 Ma. However, the scatter in the combined data sets precludes any objective elimination of points, and combining the data sets yields an upper intercept age of 997 ± 25 Ma. The mean square of weighted deviates (MSWD) is 60, indicating geologic scatter that we interpret to be a small variability in xenotime age (*22*). The slope of the Lu-Hf isochron is constrained by two xenotime fractions and the biotite fraction (Fig. 1F). Zircons and whole rocks were excluded from the regression because the zircons contain an inherited Hf component (*23*).

The Phalaborwa carbonatite (PHB) contains abundant baddeleyite needles and prismatic, greenish-gray apatite crystals. Two types of apatite were picked: large (10 mm long by 5 mm diameter) turbid crystals and small (<4 mm long by <1 mm diameter) clear crystals. Three U-Pb analyses of baddeleyite (bd-1, bd-3, and bd-4) yield a concordia age of 2059.9 ± 3.4 Ma (Fig. 1G). The large apatites are slightly discordant (+1% and −8%) and lie on or near a chord between the baddeleyite age and 0 Ma. The smaller apatites, which are more discordant (+5 to +18%) and lie substantially below the discordia, were not used for Lu-Hf analyses. Both the concordia age and the baddeleyite-apatite upper intercept age (2059.6 ± 6.6 Ma) agree well with published ages for the Phalaborwa carbonatite [2058 to 2061 Ma (*24–26*)]. A Lu-Hf isochron is defined by the two large apatites and a baddeleyite fraction (Fig. 1H). The $^{176}\text{Hf}/^{177}\text{Hf}$ ratio of the baddeleyite has been confirmed by an unspiked replicate analysis (Table 1).

The $\lambda^{176}\text{Lu}$ values determined from the four independent age comparisons are shown in Fig. 1. There is remarkable agreement among these results compared to the scatter among some of the physical counting experiments of the past two decades [e.g., (*4, 7, 8, 10*)], suggesting that the U-Pb ages and Lu-Hf slopes reflect the true crystallization ages of the minerals. Our unweighted mean results (with 2 SD uncertainties) are: $\lambda^{176}\text{Lu}(\beta^-) = 1.865 \pm 0.015 \times 10^{-11}$ year^{-1} and $t_{1/2}{}^{176}\text{Lu}(\beta^-) = 3.717 \pm 0.030 \times 10^{10}$ year. This decay constant agrees with those from the two most recent decay-counting experiments [i.e., $\lambda^{176}\text{Lu}(\beta^-) = 1.86 \pm 0.02 \times 10^{-11}$ year^{-1}, and $1.88 \pm 0.01 \times 10^{-11}$ year^{-1} (*9, 10*)]. Weighting our individual determinations by inverse variance gives a mean $\lambda^{176}\text{Lu}$ of $1.858 \pm 0.004 \times 10^{-11}$ year^{-1} with a MSWD of 0.59. This mean is strongly influenced by the Phalaborwa carbonatite, which has the smallest amount of geologic scatter of the samples. The other three samples, however, yield systematically higher $\lambda^{176}\text{Lu}$ values, and we therefore recommend the unweighted mean as the result of this study.

The existence of a minor (≤4%) decay branch of ^{176}Lu to ^{176}Yb by electron capture has been debated (*27, 28*). If it does exist, it can only contribute a maximum bias of 0.18% between counting experiment and age-comparison results (*29*). This potential bias is greatest when the oldest samples (e.g., 4.55 Ga eucrites) are used in the age comparisons. The mean age of the samples in this study is 1.3 Ga. Correcting our results for e^--capture decay would lower our $\lambda^{176}\text{Lu}(\beta^-)$ by ≤0.05%. When e^--capture is neglected in both our $\lambda^{176}\text{Lu}$ determination and in Lu-Hf age calculations, this bias cancels out for ~1.3 Ga ages, whereas Lu-Hf ages would be ≤0.13% too old for 4.56 Ga samples, and ≤0.5% too young for samples younger than 1.3 Ga. These shifts are minor relative to the present uncertainty of the decay constant, and we have therefore neglected any e^--capture when calculating our $\lambda^{176}\text{Lu}(\beta^-)$ values.

A value of $1.865 \pm 0.015 \times 10^{-11}$ year^{-1} for $\lambda^{176}\text{Lu}(\beta^-)$ requires the correction of Lu-Hf ages and many of the initial Hf isotope ratios that have been used to document the paired processes of crust formation and mantle depletion in the early Earth. Most published Lu-Hf ages are ~4% too young and therefore conclusions drawn from the comparison of Lu-Hf ages with those of other isotope systems (e.g., Sm-Nd, Rb-Sr, U-Pb) may need modification. More importantly, initial Hf isotope compositions reported for some of Earth's oldest minerals and rocks need to be recalculated. Most published initial ε_{Hf} values for early Archean zircons and evolved, low-Lu/Hf rocks shift downward by 2 to 4 ε-units when using the new $\lambda^{176}\text{Lu}$. For example, the reported $\varepsilon_{\text{Hf}}(t)$ of 0 to +4.6 for a set of early Archean gneisses and zircons from West Greenland (*30*) drops to –2.8 to +1.7 when recalculated with the new decay constant. For these low-Lu/Hf samples, most of this change is caused by the shift in the position of the chondritic uniform reservoir (CHUR) evolution curve projected back through time, rather than the shift in the initial Hf isotope composition of the sample itself. In contrast, the $\varepsilon_{\text{Hf}}(t)$ of rocks that have near-chondritic Lu/Hf will not change substantially, and rocks having superchondritic Lu/Hf will shift to higher $\varepsilon_{\text{Hf}}(t)$ values. This adjustment of $\varepsilon_{\text{Hf}}(t)$ values has significant implications for inferences regarding

Table 1. Lu-Hf data. The 2 SD external reproducibilities of $^{176}\text{Lu}/^{177}\text{Hf}$ and $^{176}\text{Hf}/^{177}\text{Hf}$ are 0.2% and 0.005%, respectively. Errors in parentheses refer to the last significant digits and are the greater of external reproducibility or 2 SE in-run statistics. Hafnium concentrations and $^{176}\text{Lu}/^{177}\text{Hf}$ take into account the variable atomic weight of Hf (i.e., from 178.5 in zircon to 176 in gadolinite). Reported $^{176}\text{Hf}/^{177}\text{Hf}$ values were adjusted for instrumental bias so that $^{176}\text{Hf}/^{177}\text{Hf}$ of JMC-475 = 0.282163.

Sample	Lu (ppm)	Hf (ppm)	$^{176}\text{Lu}/^{177}\text{Hf}$	$^{176}\text{Hf}/^{177}\text{Hf}$
		Evje (EVJ) 910.5 ± 1.6 Ma		
gd-1	4970	2.262	15,860 (1340)	272.3 (22.9)
gd-2	5549	2.498	15,490 (122)	262.8 (2.1)
gd-3	5672	2.586	15,150 (130)	260.3 (2.2)
		Tvedestrand (TVS) 1094 ± 11 Ma		
xt-2	4204	118.8	5.122 (10)	0.388416 (19)
xt-3	3844	86.35	6.474 (13)	0.416176 (21)
		Hudson Highlands (RS-1) 997 ± 25 Ma		
zrc-1 > 800 μm	174.3	15,330	0.001614 (4)	0.282363 (14)
zrc-2 < 250 μm	74.22	10,430	0.001010 (2)	0.282538 (14)
biot-2	0.7598	14.41	0.007484 (15)	0.282597 (32)
wr-1	1243	50.61	3.529 (7)	0.349371 (35)
wr-2	1315	73.46	2.564 (5)	0.330715 (56)
xt-1	2948	16.20	28.35 (7)	0.816178 (163)
xt-2	3373	19.82	26.36 (7)	0.779948 (156)
		Phalaborwa (PHB) 2059.9 ± 3.4 Ma		
bd-5	0.4702	14,280	0.00000467 (1)	0.281193 (14)
bd-6	–	–	–	0.281181 (14)
ap-2	0.3518	0.02496	2.029 (4)	0.360264 (25)
ap-3	0.4188	0.02839	2.125 (4)	0.364150 (22)

differentiation processes in the early silicate Earth and on other planetary bodies. Models based on Hf isotopes have to be revised for: (i) the ages of Earth's first enriched reservoirs, (ii) the minimum residence time of these reservoirs, and (iii) the early depletion history of Earth's mantle.

Amelin *et al.* (*31*) have noted that if a λ^{176}Lu of ~1.86×10^{-11} year^{-1} is correct, then some of Earth's oldest zircons [Jack Hills (*32*)] would indicate the existence of enriched reservoirs that had $\varepsilon_{Hf} = -3.7$ to -8.0 at 4.1 to 4.0 Ga. To produce such highly unradiogenic Hf compositions by that time, the enriched reservoir(s) (e.g., early crust) must have separated from the mantle source at or before 4.3 Ga and then survived until the zircons crystallized some 200 to 450 million years later (*31–33*). These initial Hf isotope ratios, recalculated with the new ^{176}Lu decay constant, therefore imply the existence of a differentiated silicate crust on Earth at or before 4.3 Ga. Such early crust formation in Hadean time (>4.0 Ga) is corroborated by the recently reported 4.3 to 4.4 Ga crystallization ages of the oldest preserved terrestrial zircons (*34, 35*). Short-lived isotope systems such as ^{146}Sm-^{142}Nd and ^{92}Nb-^{92}Zr [e.g. (*36–40*)] provide no compelling evidence for large-scale mantle depletion or crust formation on Earth before 4.51 Ga. In contrast to ^{92}Zr, which could develop anomalies in crustal reservoirs only until ~4.51 Ga, resolvable ^{142}Nd anomalies may have been generated in crust as late as 4.3 Ga (*38, 40, 41*). Hadean detrital minerals, which may have preserved these anomalies, have not yet been analyzed for ^{142}Nd. The available short-lived nuclide data on terrestrial rocks, together with the reevaluated Lu-Hf zircon data, suggest that Earth's first persistent crust formed between 60 and 260 million years after the condensation of the oldest solid matter in the solar system [4.566 Ga (*42*)].

References and notes

1. The value of ε_{Hf} is the deviation of the ^{176}Hf/^{177}Hf of a sample, in parts per 10^4, from that of the CHUR reference: $[(^{176}\mathrm{Hf}/^{177}\mathrm{Hf})_{sample}/(^{176}\mathrm{Hf}/^{177}\mathrm{Hf})_{CHUR} - 1] \times 10^4$. The initial ε_{Hf} or $\varepsilon_{Hf}(t)$ is the deviation from CHUR when the sample crystallized at time *t*: $\{[(^{176}\mathrm{Hf}/^{177}\mathrm{Hf})_{sample} - (^{176}\mathrm{Lu}/^{177}\mathrm{Hf})_{sample}(e^{\lambda t} - 1)]/[(^{176}\mathrm{Hf}/^{177}\mathrm{Hf})_{CHUR} - (^{176}\mathrm{Lu}/^{177}\mathrm{Hf})_{CHUR}(e^{\lambda t} - 1)] - 1\} \times 10^4$.
2. P. J. Patchett, M. Tatsumoto, *Nature* **288**, 571 (1980).
3. M. Tatsumoto, D. M. Unruh, P. J. Patchett, *Mem. Natl. Inst. Polar Res. (Tokyo)*, Special Issue no. 20, Proceedings of the Sixth Symposium on Antarctic Meteorites (December 1981), p. 237.
4. A. P. Sguigna, A. J. Larabee, J. C. Waddington, *Can. J. Phys.* **60**, 361 (1982).
5. J. Blichert-Toft, F. Albarède, *Earth Planet. Sci. Lett.* **148**, 243 (1997).
6. E. Norman, *Phys. Rev. C* **21**, 1109 (1980).
7. J. Sato, Y. Ohoka, T. Hirose, *Radiochem. Radioanal. Lett.* **58**, 263 (1983).
8. R. J. Gehrke, C. Casey, R. K. Murray, *Phys. Rev. C* **41**, 2878 (1990).
9. J. Dalmasso, G. Barci-Funel, G. J. Ardisson, *Appl. Radiat. Isotopes* **43**, 69 (1992).
10. Y. Nir-El, N. Lavi, *Appl. Radiat. Isotopes* **49**, 1653 (1998).
11. A. Boudin, S. Deutsch, *Science* **168**, 1219 (1970).
12. Analytical methods: To optimize spike-sample equilibration, all samples (except gd-2, gd-3, ap-2, and ap-3, as explained below) were spiked with ^{205}Pb-^{233}U or ^{180}Hf-^{176}Lu before digestion. To minimize error magnification effects on measured ^{176}Lu/^{177}Hf and ^{176}Hf/^{177}Hf, three different ^{180}Hf-^{176}Lu tracer solutions, covering a wide range of Lu/Hf ratios, were made. These tracers were intercalibrated against two different mixed Lu-Hf standard solutions prepared from Ames metals at Münster. Tracers for whole-rock and high-Lu/Hf samples were also cross-calibrated against two more Lu-Hf Ames metal solutions from University of California Santa Cruz (UCSC). Optimally spiked calibrations agreed with the previous Münster calibrations to within 0.2% for Lu/Hf ratios and Lu and Hf concentrations. Because the Lu/Hf of gadolinite exceeds the optimal range of our highest Lu/Hf spike, gd-2 and gd-3 were split into Hf IC, Hf ID, and Lu ID aliquots immediately after digestion, and the ID aliquots were optimally spiked for Hf and Lu, respectively. To obtain both Lu-Hf and U-Pb ages on single apatite fractions, digested ap-2 and ap-3 samples were split into a Lu-Hf aliquot and two U-Pb aliquots ("a" and "b") before spiking. Samples were digested in Savillex vials placed inside Parr Teflon bombs using HF-HNO$_3$ (zircon, baddeleyite, and biotite), 6 M HCl (apatite), HF-HCl (gadolinite), or concentrated H$_2$SO$_4$ (xenotime). Xenotime digestion was completed by periodically cooling the sample and adding concentrated HF during the H$_2$SO$_4$ evaporation step. All digested Lu-Hf samples were evaporated with HClO$_4$ to ensure complete spike-sample equilibration. Uranium and Pb were separated using a HBr anion exchange column, and their isotope compositions were analyzed on the VG Sector 54-30 TIMS at Münster. Hafnium was separated from the bulk matrix and Ti using a single ion-exchange column; the Lu+Yb cut from the Hf column was processed through an αHIBA column to remove Yb. Lutetium and Hf were analyzed in static mode on the Micromass Isoprobe at Münster. Admixed Re was used to apply an external mass bias correction to Lu. Values for the in-house Hf isotopic standard (isotope ratios indistinguishable from JMC-475) are: $^{176}\mathrm{Hf}/^{177}\mathrm{Hf} = 0.282151 \pm 6$ (2 SE, $n = 29$), $^{178}\mathrm{Hf}/^{177}\mathrm{Hf} = 1.46718 \pm 1$, $^{179}\mathrm{Hf}/^{177}\mathrm{Hf}_{raw} = 0.7367 \pm 4$, and $^{180}\mathrm{Hf}/^{177}\mathrm{Hf} = 1.88652 \pm 5$ (normalized to $^{179}\mathrm{Hf}/^{177}\mathrm{Hf} = 0.7325$ using the exponential low). All faraday cup efficiencies were set to unity.
13. J. N. Aleinikoff, R. I. Grauch, *Am. J. Sci.* **290**, 522 (1990).
14. K. R. Ludwig, *Chem. Geol.* **166**, 315 (2000).
15. Depleted mantle was modeled using present-day $\varepsilon_{Hf} = +16$ and $^{176}\mathrm{Lu}/^{177}\mathrm{Hf} = 0.04$. Here, ε_{Hf} is calculated (*1*) relative to $^{176}\mathrm{Hf}/^{177}\mathrm{Hf}_{CHUR} = 0.282772$ (*5*).
16. The low, but variable Hf blank (~30 pg ± 30%, $\mathrm{Hf}_{sample}/\mathrm{Hf}_{blank} > 1700$) accounts for a substantial portion of the ^{177}Hf in the measured Hf isotopic compositions of the gadolinites. The uncertainty of the blank correction therefore introduces a large uncertainty in the amount of ^{177}Hf present, resulting in large, correlated errors in ^{176}Lu/^{177}Hf and ^{176}Hf/^{177}Hf. Error correlations are 0.993, 0.206, and 0.315, for gd-1, gd-2, and gd-3, respectively.
17. M. A. Cosca, K. Mezger, E. J. Essene, *J. Geol.* **106**, 539 (1998).
18. F. Childe *et al.*, *Can. J. Earth Sci.* **30**, 1056 (1993).
19. R. R. Parrish, *Can. J. Earth Sci.* **27**, 1431 (1990).
20. B. S. Kamber, R. Frei, A. J. Gibb, *Precambrian Res.* **91**, 269 (1998).
21. R. K. O'Nions, H. Baadsgaard, *Contrib. Mineral. Petrol.* **34**, 1 (1971).
22. On the basis of mass balance constraints imposed by Pb isotopes, zircon and monazite impurities were ruled out as likely sources of scatter in the xenotime data. Instead, we interpret the scatter to be due to a small range in xenotime age reflecting two or more episodes of xenotime growth or partial recrystallization that occurred between two closely spaced thermal events. These events are: (i) the ~1010 Ma intrusion of the neighboring Canada Hill granite and (ii) an event at 983 Ma recorded by zircon overgrowths in the monazite-xenotime gneiss (*13*). Both events are bracketed by the 997 ± 25 Ma age, which we take to be the mean age of the xenotime in the RS-1 sample.
23. Zircons, as well as whole rocks, whose Hf isotope budgets are strongly influenced by zircon, were excluded from the regression because the zircons contain variable amounts of inherited, relatively unradiogenic Hf. This low-ε_{Hf} component is probably hosted in the obvious zircon cores. Two zircons of >800 μm size have $\varepsilon_{Hf} = -14.5$, whereas ten <250 μm grains have $\varepsilon_{Hf} = -8.3$. Excluding the zircons and whole rocks decreases isochron scatter but does not significantly change the slope.
24. L. M. Heaman, A. N. LeCheminant, *Chem. Geol.* **110**, 95 (1993).
25. T. Reischmann, *S. Afr. J. Geol.* **98**, 1 (1995).
26. I. Horn *et al.*, *Chem. Geol.* **164**, 281 (2000).
27. D. Dixon, A. McNair, S. C. Curran, *Philos. Mag.* **45**, 683 (1954).
28. R. N. Glover, D. E. Watt, *Philos. Mag.* **2**, 699 (1957).
29. The relationship between an observed experimental decay constant, λ', and the measured quantities of ^{176}Lu, ^{176}Hf* (radiogenic ^{176}Hf), and time (*t*) is $^{176}\mathrm{Hf}^*/^{176}\mathrm{Lu} = (e^{\lambda' t} - 1)$. If an e$^-$-capture branch of ^{176}Lu decay exists, the relationship between the measured quantities and the β decay constant is $^{176}\mathrm{Hf}^*/^{176}\mathrm{Lu} = (\lambda_\beta/\lambda)(e^{\lambda t} - 1)$, where λ_β is the decay constant for the ^{176}Hf*-producing β$^-$-decay branch, and λ is the total decay constant $(\lambda_\beta + \lambda_{e-})$ of ^{176}Lu. Equating the right-hand sides of these expressions and solving for λ' gives $\lambda' = \ln[(\lambda_\beta/\lambda)(e^{\lambda t} - 1) + 1]/t$. For values of *t* relevant to physical decay-counting experiments, λ' approaches λ_β. Thus, counting experiments report λ_β directly, and this result would not be affected by the existence of a minor e$^-$-capture branch. In contrast, for values of *t* relevant to age-comparison studies (e.g., 4.55 Ga for eucrites), the assumption that all ^{176}Lu decays to ^{176}Hf may cause λ' to overestimate λ_β by up to 0.18% for λ_{e-}/λ ratios up to 0.04.
30. J. D. Vervoort, J. Blichert-Toft, *Geochim. Cosmochim. Acta* **63**, 533 (1999).
31. Y. Amelin, D.-C. Lee, A. N. Halliday, *Geochim. Cosmochim. Acta* **64**, 4205 (2000).
32. Y. Amelin, D.-C. Lee, A. N. Halliday, R. T. Pidgeon, *Nature* **399**, 252 (1999).
33. The highly negative initial ε_{Hf} values of these zircons, i.e., -3.4 to -7.8 [(*31, 32*), recalculated using $\lambda^{176}\mathrm{Lu} = 1.865 \times 10^{-11}$ year^{-1}, and the CHUR parameters of Blichert-Toft and Albarède (*5*)] indicate long-term enrichment (lower Lu/Hf relative to CHUR) in the crustal sources of the zircon-bearing rocks. The time at which these source rocks were derived from a CHUR-like mantle is estimated by tracing their Hf isotope evolution curves back in time until they intersect the CHUR evolution curve. Source rocks that had granitoid-like ^{176}Lu/^{177}Hf ratios of about 0.0093 [the average of data from (*43*)], must have formed before 4.3 Ga. Amelin *et al.* (*32*) note that if the source rocks were more mafic, they would have higher ^{176}Lu/^{177}Hf ratios (e.g., 0.022), which would result in even earlier mantle separation ages. Alternatively, using newly proposed CHUR or BSE (bulk silicate Earth) reference parameters (*44–46*), or assuming that the source rocks were derived from depleted mantle rather than CHUR, would also result in even older mantle separation ages (*31, 32*). Thus, 4.3 Ga is a firm minimum age for the separation of the enriched source(s) from the mantle.
34. S. A. Wilde, J. W. Valley, W. H. Peck, C. M. Graham, *Nature* **409**, 175 (2001).
35. S. J. Mojzsis, T. M. Harrison, R. T. Pidgeon, *Nature* **409**, 178 (2001).
36. S. L. Goldstein, S. J. G. Galer, *Eos* **73**, 323 (1992).
37. C. L. Harper, S. B. Jacobsen, *Nature* **360**, 728 (1992).
38. M. T. McCulloch, V. C. Bennett, *Lithos* **30**, 237 (1993).
39. M. Sharma, D. A. Papanastassiou, G. J. Wasserburg, R. F. Dymek, *Geochim. Cosmochim. Acta* **60**, 3751 (1996).
40. C. Münker *et al.*, *Science* **289**, 1538 (2000).
41. For crust with $f_{Sm/Nd}$ values of about -0.4, where $f_{Sm/Nd} = [(^{147}\mathrm{Sm}/^{144}\mathrm{Nd})_{crust}/(^{147}\mathrm{Sm}/^{144}\mathrm{Nd})_{CHUR}] - 1$.
42. C. Göpel, G. Manhès, C. J. Allègre, *Meteoritics* **26**, 338 (1991).

43. J. D. Vervoort, P. J. Patchett, *Geochim. Cosmochim. Acta* **60**, 3717 (1996).
44. V. J. M. Salters, W. M. White, *Chem. Geol.* **145**, 447 (1998).
45. J. D. Vervoort, P. J. Patchett, J. Blichert-Toft, F. Albarède, *Earth Planet. Sci. Lett.* **168**, 79 (1999).
46. J. Blichert-Toft, N. T. Arndt, *Earth Planet. Sci. Lett.* **171**, 439 (1999).
47. Supplemental U-Pb data are available at www.sciencemag.org/fcgi/content/full/293/5530/683/DC1
48. A. H. Jaffey, K. F. Flynn, L. E. Glendenin, W. C. Bentley, A. M. Essling, *Phys. Rev. C* **4**, 1889 (1971).
49. K. R. Ludwig, *Geochim. Cosmochim. Acta* **62**, 665 (1998).
50. Deutsche Forschungsgemeinschaft funding (grant ZG 3/16) is gratefully acknowledged. We thank R. Schott for the Hudson Highlands sample, K. Cameron for providing the UCSC Ames metal Lu-Hf solutions, and T. Kleine for productive discussions. Constructive reviews from two anonymous referees are greatly appreciated.

5 April 2001; accepted 15 June 2001

Very-Long-Period Seismic Signals and Caldera Formation at Miyake Island, Japan

Hiroyuki Kumagai,[1] Takao Ohminato,[2] Masaru Nakano,[3] Masahiro Ooi,[1] Atsuki Kubo,[1] Hiroshi Inoue,[1] Jun Oikawa[2]

Over a period of roughly 40 days, starting on 8 July 2000, a caldera structure 1.7 kilometers in diameter developed by means of gradual depression and expansion of the summit crater at Miyake Island, Japan. At the same time, very-long-period (VLP) seismic signals were observed once or twice a day. Source mechanism analyses of the VLP signals show that the moment tensor solutions are smooth step functions over a time scale of 50 seconds, with dominant volumetric change components. We developed a model to explain the caldera and the VLP signals, in which a vertical piston of solid materials in the conduit is intermittently sucked into the magma chamber by lateral magma outflow. This model offers potential for making quantitative estimations of the characteristic physical properties of magma systems.

On Miyake Island (Fig. 1A), one of the Izu volcanic islands of Japan, quasiperiodic eruptions of basaltic magma have been recorded since 1085 A.D. (*1*). Three eruptions occurred in 1940, 1962, and 1983, with a roughly 20-year interval and producing 10^7 m^3 of erupted materials during each eruption (*2*). On 26 June 2000, an earthquake swarm beneath the island and anomalous changes of tiltmeters on the island indicated that magma intruded close to the surface along the southwestern flank (*3*). However, an eruption did not occur at that time and the earthquake swarm migrated toward Kozu Island, 40 km northwest of Miyake Island (Fig. 1A). On 8 July the first eruption occurred at the summit crater of Miyake Island, and the depression of the summit crater began. The summit crater gradually sank and expanded until the middle of August, leaving a caldera 1.7 km in diameter (Fig. 1B) (*4*). At the same time, very-long-period (VLP) seismic signals were observed once or twice a day between 11 July and 18 August. During most of this period, there were only small eruptions, accompanied by ash ejections from the summit. The size of the summit eruptions increased gradually after 11 August, and the largest eruption that has occurred so far took place on 18 August. Sulfur dioxide (SO_2) gas emissions from the summit started on 29 August and have continued for more than 9 months. In contrast to the heightened SO_2 gas emissions, the earthquake swarm between Miyake and Kozu Islands gradually decreased after the largest eruption on 18 August.

The VLP signals showed similar impulsive waveforms (Fig. 2A), suggesting a repetitive and nondestructive source process. The VLP signals are not directly associated with eruptions but rather with a steplike inflation, followed by slow deflation recorded by the tiltmeters on the island (*3*). Source mechanism analyses of the VLP signals recorded by the Japanese broadband seismometer network (FREESIA/KIBAN) and a temporary seismic station on the island show that the source time functions of the moment tensor are represented by a smoothed step function over a

---

[1] National Research Institute for Earth Science and Disaster Prevention, Tsukuba, Japan. [2] Earthquake Research Institute, University of Tokyo, Tokyo, Japan. [3] Graduate School of Environmental Studies, Nagoya University, Japan.

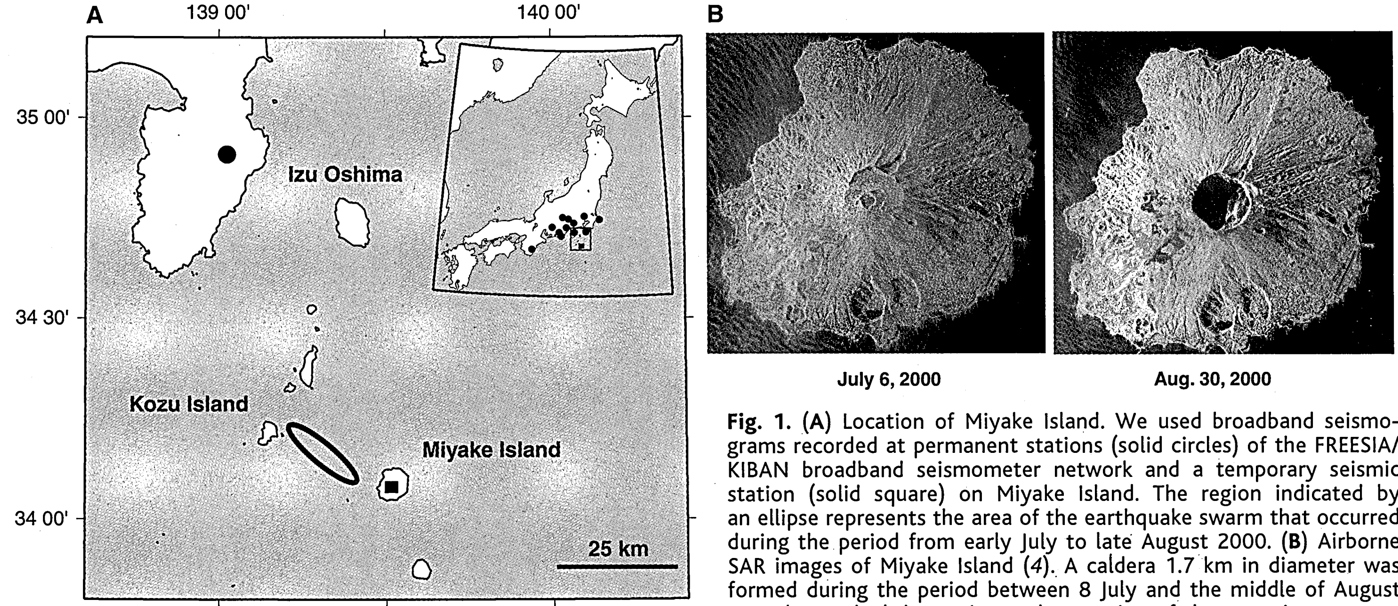

July 6, 2000

Aug. 30, 2000

Fig. 1. (**A**) Location of Miyake Island. We used broadband seismograms recorded at permanent stations (solid circles) of the FREESIA/KIBAN broadband seismometer network and a temporary seismic station (solid square) on Miyake Island. The region indicated by an ellipse represents the area of the earthquake swarm that occurred during the period from early July to late August 2000. (**B**) Airborne SAR images of Miyake Island (*4*). A caldera 1.7 km in diameter was formed during the period between 8 July and the middle of August 2000 by gradual depression and expansion of the summit crater.